OPEN ACCESS

International
Journal
Of Modern Engineering Research (IJMER)

Design and Manufacture of a High Resolution Orbital-Trapping Mass-Analyser for Secondary Ion Mass Spectrometry

James C. Hood and Peter J. Cumpson
School of Mechanical and Systems Engineering, Newcastle University, Newcastle-upon-Tyne, NE1 7RU, U.K.

ABSTRACT *We have designed and fabricated a high mass-resolution orbital trapping analyser for Secondary Ion Mass Spectrometry (SIMS). A key issue is the precise machining and alignment of components of the ion trap. We perform finite difference method (FDM) simulations and ion trajectory calculations to establish the precision needed in manufacturing and aligning the trap. Machining of the high-precision mathematically-defined electrode surface was achieved through the use of hand-crafted G-code segments. The ion trap and transfer assembly, once assembled, were characterized and key dimensions measured, these then being used for simulations of ion trajectories to check the operation of the device.*

Keywords: *Secondary ion mass spectrometer, ion trap, precision machining, surface analysis*

I. INTRODUCTION

Secondary Ion Mass Spectrometry (SIMS) is a key technique in the characterization of surface chemistry in a wide range of technological applications, from advanced coatings, medical implant surfaces, pharmaceutical characterization, semiconductor fault-finding and many other applications [1]. Briefly, a SIMS instrument consists of an ion source producing monoenergetic ions, a sample surface under analysis, and a mass analyser to detect and to a certain extent quantify the charged fragments produced.

A persistent problem in SIMS has been the ambiguities that arise due to the multiplicity of peaks that appear in SIMS spectra. Whereas in some applications (notably semiconductor work) peaks can often be attributed unambiguously to certain chemical species through prior knowledge of what these are likely to be, there are many applications (notably medical and biological ones) where the origin of the surface chemistry is complex and often poorly-understood, at least initially. This often leads to a very large number of peaks in each SIMS spectrum, with little prior information to guide their assignment to particular species. Even experts in SIMS interpretation are seldom able to assign species to all the peaks in a spectrum with great confidence.

Secondary ions can be more uniquely identified through mass-spectroscopy/mass-spectroscopy (MS/MS) to help resolve this ambiguity by first mass filtering then breaking up the ions and performing mass spectroscopy on the resulting fragments. However this technique has not generally been available in SIMS instruments until recently [2,3]. Equally important is improved mass resolution in SIMS spectra, which would allow greater confidence in peak attribution due to the mass defects of the component atoms in the ion, effectively identifying those atoms by their small deviations from unit atomic masses. One cannot generally distinguish isomers in this way (for this MS/MS remains extremely valuable) but molecules having the same nominal unit mass often can be distinguished using mass defects alone. Higher mass resolution in SIMS would allow for the removal of ambiguity in the case of separating hydrides from element peaks in cosmochemistry [4], for example, as well as many other practical and technological applications. Mass resolution in excess of the 10,000 attainable with modern ToF-SIMS instruments is required to distinguish between metal hydrides and element peaks for masses higher than 100 atomic mass units, as shown by the dashed line in Figure 1.

There have been a number of developments that aim to improve greater mass resolution in SIMS. Examples include an Ion Cyclotron Resonance (ICR-MS) analyser that holds the record to date for SIMS mass resolution to our knowledge [5,6]. Alternative Fourier-Transform mass spectrometers have previously been coupled with SIMS instruments in the past [7,8]. More recently the Iontof company has developed a hybrid instrument by connecting an Iontof V ToF-SIMS instrument to a commercially-available Thermo Orbitrap™ mass

spectrometer [9]. Inevitably there are compromises when connecting different instruments originally designed to operate differently. In contrast, our aim was to develop a new mass analyser closely-integrated with an existing Ionoptika J105 SIMS instrument, and indeed our analyser was designed and constructed here at Newcastle University while we were awaiting delivery of that instrument from the manufacturer.

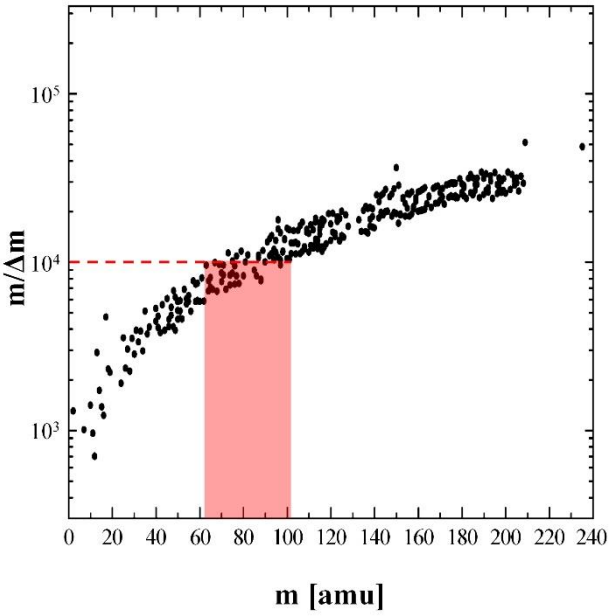

Figure 1: Mass resolution required to separate hydrides from elemental peaks – adapted from [4]. Clearly a mass resolution above 10,000 is needed to identify hydrides above around 100 atomic mass units (amu).

II. FABRICATION CHALLENGE

Our analyser design is based on the axially-harmonic orbital ion trap proposed by Makarov [10]. This, being an electrostatic trap, does not require expensive high-field magnets of the type used in ICR-MS. Briefly, the ion trap works by applying a potential between an internal "spindle" electrode and two external electrodes held at (virtual) earth potential. Ions injected into the trap follow complex orbits, but Makarov showed that in terms of their axial displacement they follow harmonic paths whose frequency depends on the ion mass-to-charge ratio. These oscillations can be detected and quantified using a sensitive differential charge amplifier connected to the two outer electrodes – essentially measuring the "image charges" induced in those electrodes in response to the ions oscillating in the trap. The disadvantage of this orbital ion trap (compared to ICR-MS for example) is the accuracy of the electric field that needs to be applied between the electrodes, and therefore the high level of accuracy needed in the machining and aligning of those electrodes. As we shall see, this accuracy can be on the scale of a few micrometres, or even less.

The precision required in the manufacture and assembly of the ion trap electrodes was determined through finite difference method (FDM) simulations using the commercially available software package, SIMION 8.1[11].

In total 8 different modes of misalignment were simulated, as listed in Table 1, with the axes of the ion trap defined as in Figure 2. For each simulation, ten ions with mass difference of 0.1u (where u represents one atomic mass unit) were flown. A greater number of ions would have been too computationally expensive, and ten were sufficient to obtain basic statistics. The 'output' mass of each ion was evaluated from the ion's axial oscillation frequency, as laid out in [10]. The mass resolution attainable for various misalignments was found by comparing the calculated 'output' mass with that obtained from an ideal simulation without any misalignment, as shown in Eqn (1), where R is mass resolution, m_{input} is the input mass, m_{ref} is the calculated mass from the reference simulation and $m_{misalignment}$ is the calculated mass from the misaligned simulation.

Table 1: Simulated misalignments

Type of Misalignment	Axis of Misalignment / Centre of Rotation	Electrode
Displacement	z-axis	Internal
Displacement	z-axis	External
Displacement	r-axis	Internal
Displacement	r-axis	External
Rotation	Mid-point	Internal
Rotation	Mid-point	External
Rotation	End-point (P)	Internal
Rotation	End-point (P)	External

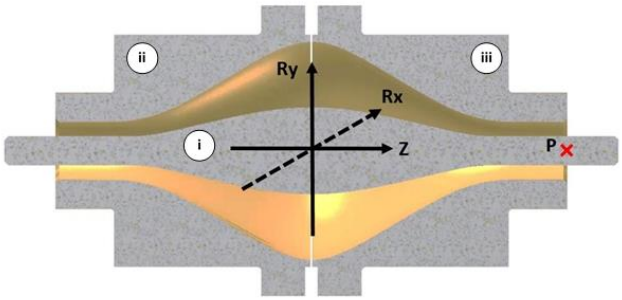

Figure 2: Ion trap axes, where i) is the internal "spindle" electrode, and ii) & iii) are the external electrodes

$$\boldsymbol{R = \frac{m}{\Delta m} = \frac{m_{input}}{m_{ref} - m_{misalignment}}} \tag{1}$$

The two principal misalignments examined were axial displacement of the internal and external electrodes relative to one another, results for which can be found in Figure 3 and Figure 4. Misalignment of this type could arise during machining, for example if an incorrect or imprecise datum is used, or during assembly of the ion trap if component interfaces are damaged or otherwise made to function improperly. It was found that the maximum allowable axial misalignment of the internal electrode was 99.5µm to achieve mass resolution of 10,000, the tolerable axial misalignment for the external electrodes was found to be much lower at only 1.5µm for mass resolution of 10,000, as shown in Table 2.

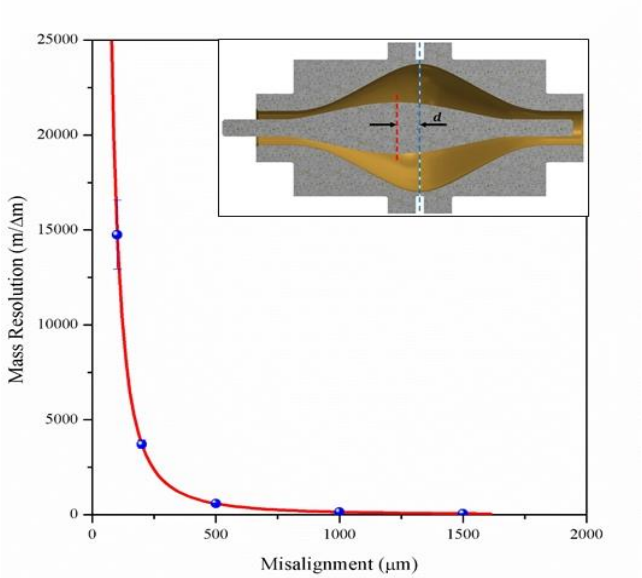

Figure 3: Internal electrode axial misalignment simulated mass resolution results with computer-aided-design (CAD) model of exaggerated misalignment inset

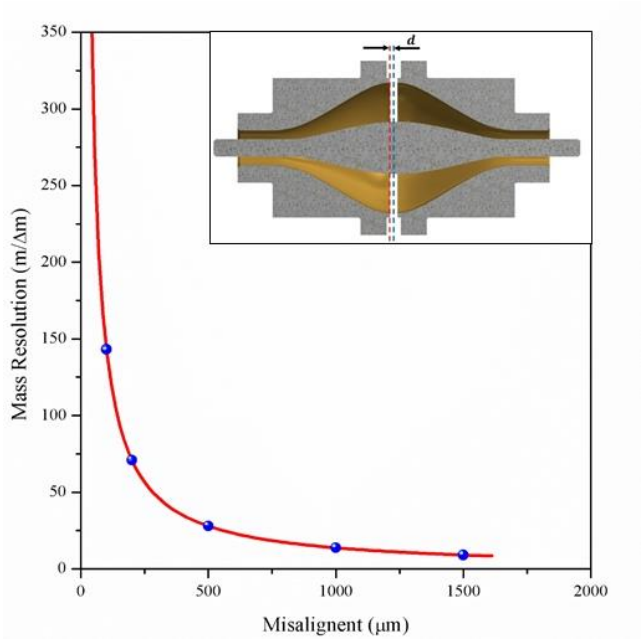

Figure 4: External electrode axial misalignment simulated mass resolution results with CAD model of exaggerated misalignment inset

Table 2: Axial misalignment simulation results

Axial Misalignment	**Misalignment for m/Δm = 10,000**	**Misalignment for m/Δm = 100,000**
Internal Electrode	99.5μm	31.5μm
External Electrode	1.5μm	0.2μm

The increased sensitivity to misalignment of the external electrode can be explained by the increased air-gap, this break in the electric field will cause a much greater perturbation in the ideal electrostatic potential than a simple translation of the internal electrode.

III. COMPUTER NUMERICALLY CONTROLLED MACHINING

As confirmed by the misalignment simulations, there is very little margin for error in the manufacture and assembly of the ion trap electrodes, therefore accurate machining was of paramount importance. The ideal profile of the electrodes is of a quadro-logarithmic form, as described by Eqn (2), from Makarov [10].

$$z(r) = \sqrt{\frac{r^2}{2} - \frac{\left(R_{1,2}\right)^2}{2} + (R_m)^2 \cdot \ln\left(\frac{R_{1,2}}{r}\right)} \tag{2}$$

To translate this relationship into a computer numerically controlled (CNC) machining compatible "G-code" required for manufacture, a number of tools were utilised, including in-house written MATLAB scripts and CAD software. One issue in turning a complex profile such as this on a CNC machine is maintaining the mathematical smoothness of the operation, if G-code is written without considering this it can result in discontinuities in the piecewise representation of the continuous function. Therefore, in this case tangent arcs were used to approximate the ideal electrode profile whilst preserving its smoothness in the form of G^1 continuity [12].

The accuracy of the G-code approximation of the electrode profile was then evaluated using our own code written in MATLAB, with Figure 5 showing the two profiles overlaid for the internal electrode, in this plot almost no discrepancies can be seen visually. To investigate errors between the curves which are not visible in

Figure 5, the G-code profile was subtracted from the ideal electrode profile in MATLAB, resulting in the error plot shown in Figure 6.

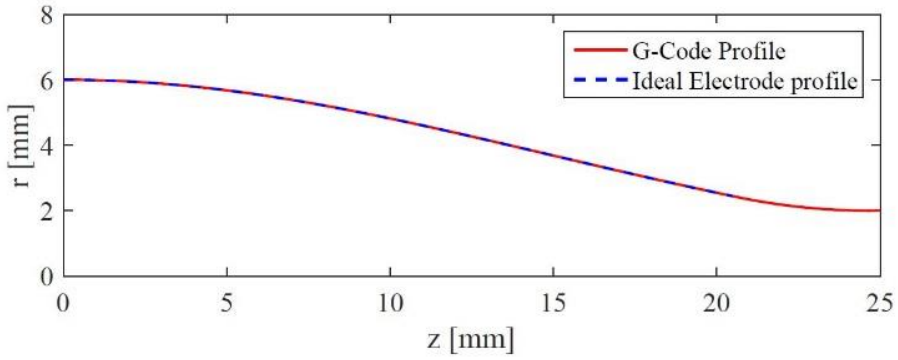

Figure 5: Overlay of ideal internal electrode profile with G-code approximation

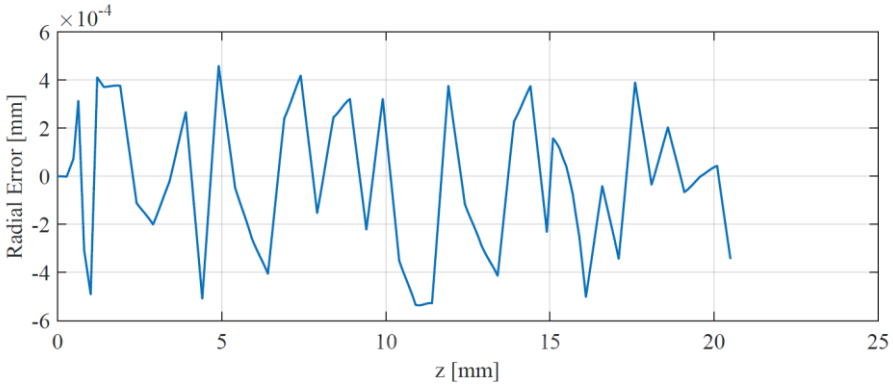

Figure 6: Resulting radial error when G-code profile is subtracted from ideal internal electrode profile

It can be seen that the maximum radial error for the internal electrode was less than 0.6µm in magnitude, the maximum radial error for both internal and external electrodes is shown in Table 3.

Table 3: Maximum radial error between G-code and ideal electrode profiles

	Internal Electrode	**External Electrode**
Maximum Radial Error	-0.536µm	+0.473µm
Axial Position of Max. Error	z = 11mm	z = 8.5mm

In theory, an arbitrarily small value for radial error could be obtained by increasing the number of arcs used to approximate the ideal profile. However, as the CNC milling machine used accepts input only to the nearest micron, this is not the case in practice. The disadvantage of using a greater number of arcs would be the increase in time required to evaluate the arcs computationally, with diminishing returns in the reduction of radial errors.

IV. ION TRAJECTORY SIMULATION

Further SIMION simulations were performed to optimise the transfer of ions into the new mass analyser and confirm the conditions required for their successful trapping, as demonstrated in the simulations screenshots in Figure 7. These screenshots represent an ideal capture of a single ion, resulting in the perfectly circular radial orbit as shown in Figure 7 ii).

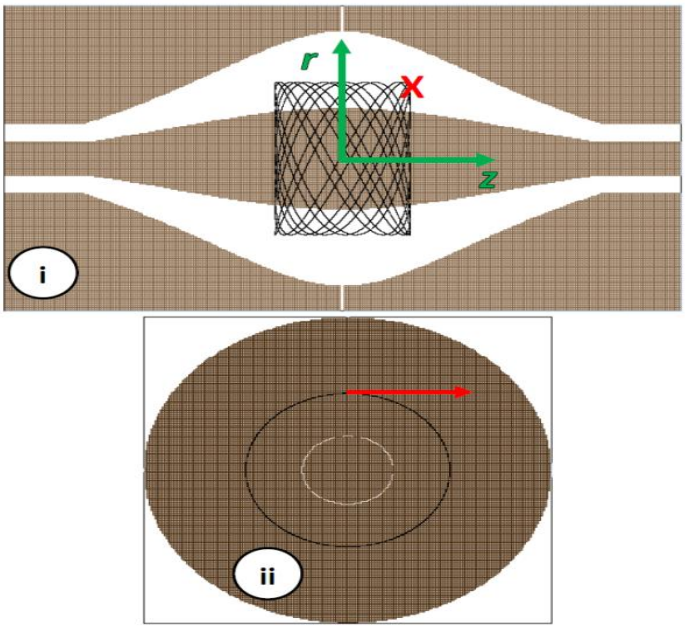

Figure 7: Simulated ideal ion trajectories within ion trap; i) axial view ii) radial view

The simulation of different voltages applied to elements of the ion transfer optics was an essential step in predicting the optimal conditions to successfully transfer ions from the J105 instrument to the mass analyser. A simplified model showing successful ion transfer and capture is shown in Figure 8. In the simulations used to model ion transfer, 300 ions were flown in each run so as to account for multiple ion initial conditions simultaneously, thus giving an estimate for the percentage of ions successfully transferred into the mass analyser. This large number of simulated ions (compared to the number used in earlier studies) was possible due to a coarser simulation time-step being used than for the misalignment simulations. A larger time-step was permissible as mass resolution was not being evaluated from ion trajectories in this instance. The ions were grouped into 3 distinct sets of initial conditions exiting the J105 SIMS, each with different starting co-ordinates but equivalent conical velocity distributions. In total, over 120 simulations were run to optimise transfer voltages, with maximum simulated ion transmission from the J105 SIMS to the mass analyser in excess of 50%.

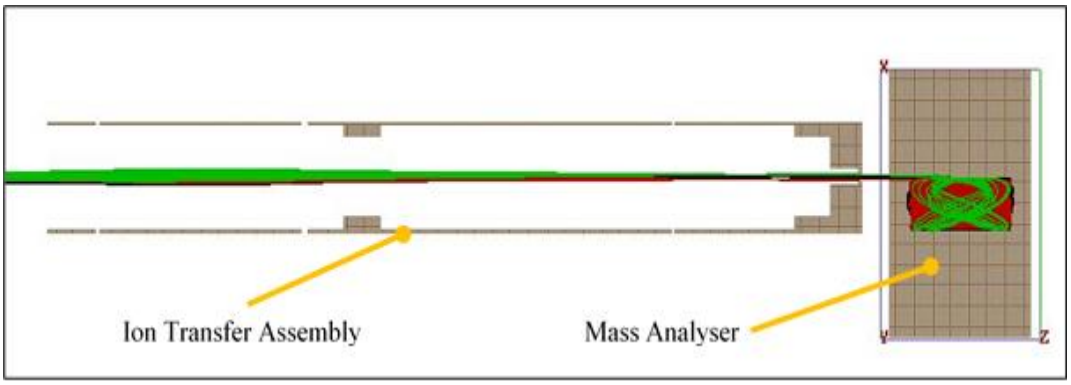

Figure 8: Simplified SIMION model of ion transfer optics and mass analyser. The outlines of the inner and outer electrodes are not shown for the purposes of clarity. Red, black and green ion trajectories represent ions simulated with different initial conditions.

Once successful ion transfer had been simulated, the CAD model was adjusted to reflect the optimum arrangement of ion transfer components, the transfer assembly was then constructed accordingly. The assembled analyser and associated ion transfer optics are shown in Figure 9 mounted onto the J105 SIMS, alongside a CAD model of the transfer and ion trap assembly.

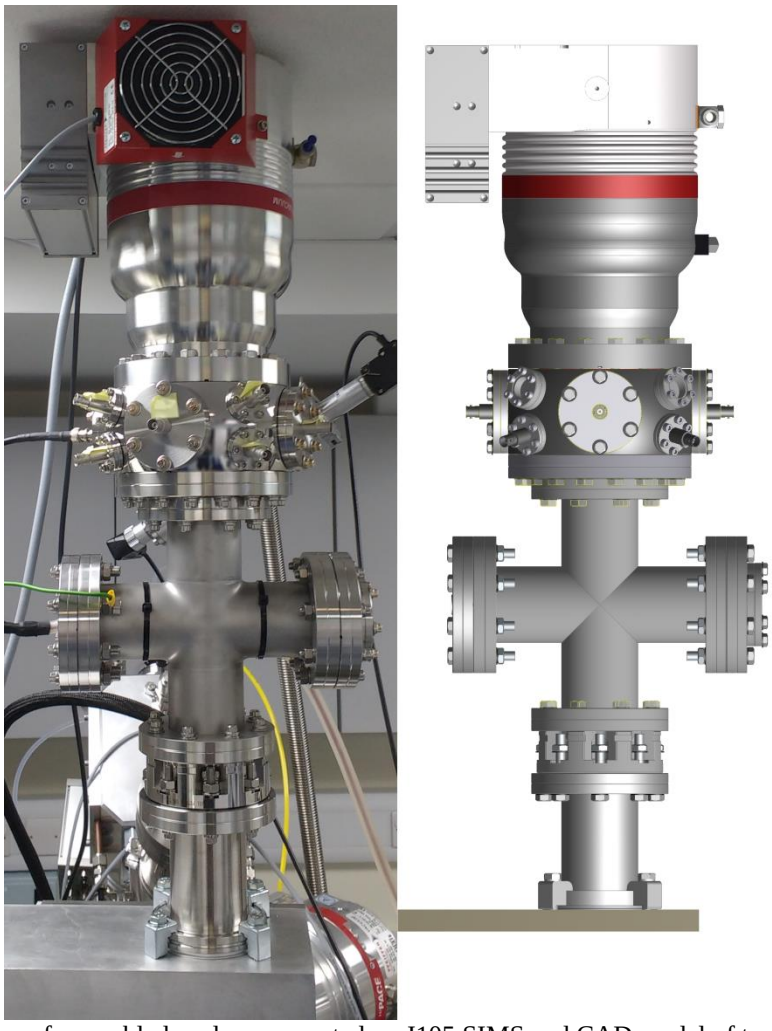

Figure 9: Comparison of assembled analyser mounted on J105 SIMS and CAD model of transfer assembly

V. FUTURE WORK

The performance of the mass analyser in service will be reported elsewhere. The next major steps forward for this project are as follows:

1. Cryogenic reduction of electronic noise

Commercial SIMS analysers typically operate at room temperature, whereas ICR-MS instruments typically use superconducting magnets that need to be maintained at cryogenic temperatures. One of the advantages of cryogenic operation is that the ion detection electronics, which has the extremely challenging task of measuring very small currents, is also cooled to a low temperature, greatly reducing thermal noise. In the context of ToF-SIMS of organic samples, liquid nitrogen is regularly used to cool samples in ultra-high-vacuum (UHV) and is therefore readily available nearby, so the trap was designed so as to allow cooling of the detection electronics by liquid nitrogen. In principle a closed-cycle helium cryostat could also be used, but we anticipate that liquid nitrogen alone will provide a major advantage in terms of reducing the ion detection limit.

2. Improving cluster ionization yield

A key issue limiting the spatial resolution is the ion yield. Without ionizing a larger fraction of the secondary species than is usually the case, there are simply not enough ions produced by impacts at the 10-100nm scale at which we would wish to analyse in many contexts. We anticipate the use of water clusters will be crucial here, as they have been demonstrated to improve ion yield by a factor of more than 10 in comparison to argon cluster sources [13,14], greater ion yield such as this is key to achieving high mass-resolution at high spatial resolution.

VI. CONCLUSION

We have designed, simulated and constructed a high mass-resolution analyser for the J105 imaging SIMS instrument. Rigorous accuracy requirements for machining the complex surfaces, especially of the inner trapping electrode, were estimated by ion trajectory simulations and have been overcome by careful low-level programming of G-code for CNC tooling. The design and assembly of ion optic components have been informed by ion trajectory simulations to optimise transfer of ions into the mass analyser, with over 50% transmission achieved in simulation.

Acknowledgements

We are extremely grateful to the team of students and staff at Newcastle University that have worked on this project since 2013 in the form of an MSc project, masters student group project and summer scholarship projects, notably (and in alphabetical order) Nicholas Burn, Jack Calder, Joseph Ford, Andrew Kiang, Lisa Li, Joe Midgley, Jonathan Rhodes, Grant Saunby and Siyao Xu. Mr Stuart Baker and Mr Jamie Hodgson of the CNC workshop in the School of Mechanical Engineering deserve particular thanks, and especially to Mr Mike Foster for a very high level of support throughout this project. Thanks to Dr Barry Gallacher for some of the detection and digitization electronics, and Mr Richard Burnett for electronics advice. Finally we thank Mr Paul Blenkinsopp of Ionoptika Ltd for giving access to detailed drawings of the J105 instrument to facilitate our work. Purchase of the J105 instrument was funded in part by the EPSRC Great Eight Technologies capital grant EP/K022679/1, and in part by Newcastle University, to both of which the authors are very grateful.

REFERENCES

[1]. A.M. Belu, D.J. Graham, D.G. Castner. Time-of-flight secondary ion mass spectrometry: Techniques and applications for the characterization of biomaterial surfaces, *Biomaterials*, *24*(*21*), 2003, 3635–3653.

[2]. J.S. Fletcher, S. Rabbani, A. Henderson, P. Blenkinsopp, S.P. Thompson, N.P. Lockyer, J.C. Vickerman. A New Dynamic in Mass Spectral Imaging of Single Biological Cells, *Analytical Chemistry*, *80*(*23*), 2008, 9058–9064.

[3]. G.L. Fisher, J.S. Hammond, P.E. Larson, S.R. Bryan, R.M.A. Heeren. Parallel imaging MS/MS TOF-SIMS instrument, *Journal of Vacuum Sciene & Technology B*, *34*(*3*), 2016, 03H126.

[4]. T. Stephan. ToF-SIMS in Cosmochemistry, *Planetary and Space Science*, *49*(*9*), 2001, 859–906.

[5]. S. Maharrey, R. Bastasz, R. Behrens, A. Highley, S. Hoffer, G. Kruppa, J. Whaley. High mass resolution SIMS, *Applied Surface Science*, *231–232*, 2004, 972–975.

[6]. D.F. Smith, E.W. Robinson, A. V Tolmachev, R.M.A. Heeren, L. Pa, L. Pasa-Tolic. C60 Secondary Ion Fourier Transform Ion Cyclotron Resonance Mass Spectrometry, *Analytical Chemistry*, *83*(*24*), 2011, 9552–9556.

[7]. M.E. Castro, D.H. Russel. Cesium Ion Desorption Ionization with Fourier Transform Mass Spectrometry, *Analytical Chemistry*, *56*(*3*), 1984, 578–581.

[8]. I.J. Amster, J.A. Loo, J.J.P. Furlong, F.W. Mclafferty. Cesium Ion Desorption Ionization with Fourier Transform Mass Spectrometry, *Analytical Chemistry*, *59*(*20*), 1987, 313–317.

[9]. A. Pirkl, R. Moellers, H. Arlinghaus, F. Kollmer, E. Niehuis, A. Makarov, S. Horning, M. Passarelli, R. Havelund, P. Rakowska, A. Race, A.G. Shard, A. West, P. Marhsall, C.F. Newman, M. Alexander, C. Dollery, I.S. Gilmore. A Novel Hybrid Dual Analyzer SIMS Instrument for Improved Surface and 3D-Analysis, *Microscopy and Microanalysis*, *22*(*Suppl 3*), 2016, 340–341.

[10]. A. Makarov. Electrostatic axially harmonic orbital trapping: A high-performance technique of mass analysis, *Analytical Chemistry*, *72*(*6*), 2000, 1156–1162.

[11]. D.A. Dahl. SIMION for the personal computer in reflection, *International Journal of Mass Spectrometry*, *200*, 2000, 3–25.

[12]. B.A. Barsky, T.D. DeRose. Geometric Continuity of Parametric Curves: Constructions of Geometrically Continuous Splines, *IEEE Computer Graphics and Applications*, *10*(*1*), 1990, 60–68.

[13]. S. Sheraz née Rabbani, A. Barber, J.S. Fletcher, N.P. Lockyer, J.C. Vickerman. Enhancing secondary ion yields in ToF-SIMS using water cluster primary beams, *Analytical chemistry*, *85*, 2013, 5654–5658.

[14]. S. Sheraz née Rabbani, I.B. Razo, T. Kohn, N.P. Lockyer, J.C. Vickerman. Enhancing ion yields in time-of-flight-secondary ion mass spectrometry: A comparative study of argon and water cluster primary beams, *Analytical Chemistry*, *87*(*4*), 2015, 2367–2374.